Supplemental Material to the Manuscript: "Efimov States of Strongly Interacting Photons"

I. TWO-BODY SCATTERING WITH ANISOTROPIC MASS

In this section we compare the scaling of the T-matrix elements with energy for the higher-partial waves in the two-body problem with an anisotropic mass to the Born approximation.

The Schrödinger equation for the wavefunction of two dark-state polaritons (branch $\mu = D$) with identical anisotropic masses in the rescaled coordinates defined in the main text is

$$-\frac{\tilde{\nabla}^2\psi}{m} + U(\tilde{r},\tilde{\theta})\psi = E\psi, \tag{S1}$$

$$U(\tilde{r},\tilde{\theta}) = -\frac{\alpha/\bar{\chi}[2\epsilon_D(\boldsymbol{q}_0)]}{1+\frac{\tilde{r}^6}{r_0^6}\left(1+\frac{\cos^2\tilde{\theta}\cos 2\beta}{\sin^2\beta}\right)^3}, \tag{S2}$$

$$\bar{\chi}(\omega) = \frac{\Delta-\omega/2-\frac{\Omega^2}{\Delta-\omega}}{\omega(\Delta-\omega/2)+2\Omega^2},\ \alpha \approx |S_D^{\boldsymbol{q}_0}|^4, \tag{S3}$$

$$|S_\mu^{\boldsymbol{q}}|^2 = \frac{\Omega^2}{\Omega^2+\epsilon_\mu(\boldsymbol{q})^2}, \tag{S4}$$

where $\boldsymbol{q}_0$ is the incoming momentum of the two dark-state polaritons and $S_\mu^{\boldsymbol{q}}$ is the overlap of the single polariton eigenstate on branch μ with momentum $\boldsymbol{q}$ with the Rydberg state. Expanding the wavefunction in spherical harmonics and dropping the tildes over the rescaled coordinates

$$\psi = \frac{1}{r}\sum_{\ell,m} Y_{\ell m}(\theta,\phi) f_{\ell m}(r), \tag{S5}$$

we arrive at the radial Schrödinger equation

$$-\frac{f''_{\ell m}}{m} + \frac{\ell(\ell+1)}{mr^2} f_{\ell m} + \sum_{\ell'} U^{(m)}_{\ell\ell'}(r) f_{\ell' m} = E f_{\ell m}, \tag{S6}$$

$$U^{(m)}_{\ell\ell'}(r) = 2\pi\int_0^\pi \sin\theta d\theta\, Y^*_{\ell m}(\theta,\phi) U(r,\theta) Y_{\ell' m}(\theta,\phi), \tag{S7}$$

with the boundary conditions [S1]

$$\lim_{r\to 0} f^{\ell' m}_{\ell m}(r) = 0, \tag{S8}$$

$$\lim_{r\to\infty} f^{\ell' m}_{\ell m}(r) = \delta_{\ell\ell'} e^{-i(kr-\frac{\ell'\pi}{2})} - S^{(m)}_{\ell\ell'} e^{i(kr-\frac{\ell'\pi}{2})}. \tag{S9}$$

Here $k=\sqrt{mE}$ and $S^{(m)}_{\ell\ell'}$ is the multi-channel S-matrix, which has to be found self-consistently.

In the first Born approximation the scattering amplitude defined in Eq. (9) of the main text takes the form

$$f(\hat{k}_i,\hat{k}_f) = -\frac{1}{2\pi}\int d^3 r e^{i\boldsymbol{k}_i\cdot\boldsymbol{r}} U(r,\theta) e^{-\boldsymbol{k}_f\cdot\boldsymbol{r}}. \tag{S10}$$

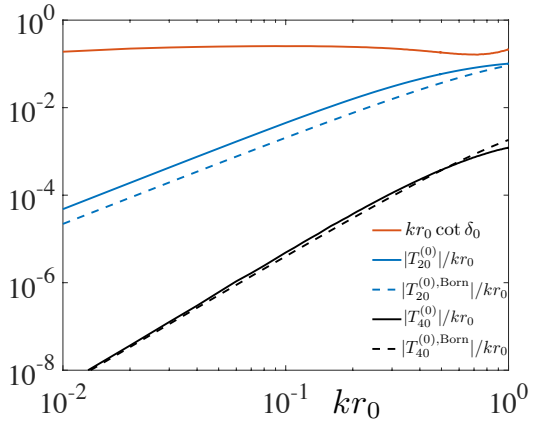

FIG. S1: (a) Scaling of T-matrix elements as a function of $k=\sqrt{mE}$. Near threshold, the scattering is dominated by the diagonal s-wave component $S_{00}^{(0)} = e^{i\delta_0(k)}$, which defines the scattering length via $k\cot\delta_0 = -1/a + O(k^2)$. Here we took $\sqrt{mU(0)}r_0 = 2.2$ and $m_\perp/m_z = 20$.

Using the expansion of $e^{i\boldsymbol{k}\cdot\boldsymbol{r}}$ into spherical harmonics, this equation directly implies that

$$T^{(m),\mathrm{Born}}_{\ell\ell'} = -k\Gamma^{(m)}_{\ell\ell'}, \tag{S11}$$

$$\Gamma^{(m)}_{\ell\ell'} = -4\int r^2 dr j_\ell(kr) j_{\ell'}(kr) U^{(m)}_{\ell\ell'}(r), \tag{S12}$$

where $j_\ell(x)$ are spherical Bessel functions. For an interaction potential that dies off as $1/r^s$, $T^{(m),\mathrm{Born}}_{\ell\ell'}$ has the scaling given in Eq. (10) of the main text. We have verified these scalings for the higher partial wave S-matrix elements using numerical solutions of the radial Schrödinger equation. An example is shown in Fig. S1(a) for the s-wave channel with a large mass ratio of $m_\perp/m_z = 20$. In Fig. 2(c) of the main text we obtained the scattering length through numerical solutions of the S-matrix including the $\ell = 0$ and $\ell = 2$ partial wave channels. We further verified that including the $\ell = 4$ channel had a negligible effect on the position of the s-wave scattering resonances, which is consistent with the perturbative analysis in Sec. III.

II. SCALING OF THREE-BODY LOSS RATE

In this section, we derive the scaling of the three-body loss rate near the EIT resonance for large values of the interaction parameter $\phi = g^2 r_b/c\Delta = \mathrm{OD}_b\gamma/\Delta$, where OD_b is the optical depth per blockade radius.

From the optical theorem, the three-body loss appears as an imaginary contribution to the self-energy

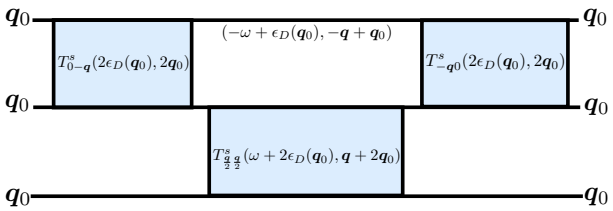

FIG. S2: One-loop contribution to the three-body T-matrix with all incoming and outgoing states dark-state polaritons at the same momentum. The imaginary part of this diagram gives the lowest order contribution to the three-body loss rate.

of three dark-state polaritons [S2]. Thus we can find the lowest order contribution to the three-body loss rate in the two-body T-matrix by evaluating the imaginary part of the diagram in Fig. S2, which contains a single loop. In this diagram the shaded boxes represent the symmetrized two-particle T-matrix $T^s_{\boldsymbol{k}\boldsymbol{k}'}(\omega, K) = [T_{\boldsymbol{k}\boldsymbol{k}'}(\omega, \boldsymbol{K}) + T_{\boldsymbol{k}-\boldsymbol{k}'}(\omega, \boldsymbol{K})]/2$, where ω and $\boldsymbol{K} = \boldsymbol{q}_1 + \boldsymbol{q}_2$ are the total energy and momentum of the incoming polaritons with momenta $\boldsymbol{q}_{1,2}$, respectively, $\boldsymbol{k} = (\boldsymbol{q}_1 - \boldsymbol{q}_2)/2$ is the incoming relative momentum of the two polaritons, and $\boldsymbol{k}'$ is the outgoing relative momentum. The solid lines are the time-ordered, non-interacting Green's function for a single Rydberg state

$$g^{\boldsymbol{q}}_s(\omega) = \sum_\mu \frac{|S^{\boldsymbol{q}}_\mu|^2}{\omega - \epsilon_\mu(\boldsymbol{q}) + i\epsilon}, \tag{S13}$$

where $S^{\boldsymbol{q}}_\mu$ is the overlap of the single polariton eigenstate on branch μ with momentum $\boldsymbol{q}$ with the Rydberg state. Using these Feynman rules and performing the integral over the virtual frequency ω, the diagram in Fig. S2 evaluates to

$$\int \frac{d^3q}{8\pi^3} \sum_{\mu,\nu,\gamma} |S^{\boldsymbol{q}_0-\boldsymbol{q}}_\mu|^2 |S^{\boldsymbol{q}_0+\boldsymbol{q}}_\nu|^2 |S^{\boldsymbol{q}_0+\boldsymbol{q}}_\gamma|^2 \frac{T^s_{0-\boldsymbol{q}}(2\epsilon_D(\boldsymbol{q}_0), 2\boldsymbol{q}_0) T^s_{\frac{\boldsymbol{q}}{2}\frac{\boldsymbol{q}}{2}}(3\epsilon_D(\boldsymbol{q}_0) - \epsilon_\mu(\boldsymbol{q}_0-\boldsymbol{q}), 2\boldsymbol{q}_0+\boldsymbol{q}) T^s_{-\boldsymbol{q}0}(2\epsilon_D(\boldsymbol{q}_0), 2\boldsymbol{q}_0) |S^{\boldsymbol{q}_0}_D|^6}{[2\epsilon_D(\boldsymbol{q}_0) - \epsilon_\mu(\boldsymbol{q}_0-\boldsymbol{q}) - \epsilon_\nu(\boldsymbol{q}_0+\boldsymbol{q})][2\epsilon_D(\boldsymbol{q}_0) - \epsilon_\mu(\boldsymbol{q}_0-\boldsymbol{q}) - \epsilon_\gamma(\boldsymbol{q}_0+\boldsymbol{q})]}. \tag{S14}$$

Neglecting the contribution from two-body poles, the only genuine three-body poles in the integrand appear in $T^s_{\frac{\boldsymbol{q}}{2}\frac{\boldsymbol{q}}{2}}(3\epsilon_D(\boldsymbol{q}_0) - \epsilon_\mu(\boldsymbol{q}_0-\boldsymbol{q}), 2\boldsymbol{q}_0+\boldsymbol{q})$. When there are deep two-body bound states, the pole will appear at low virtual momentum. Evaluating the integral over this pole will give the lowest order contribution to the three-body recombination rate. In the absence of two-body bound states, the only poles in $T^s_{\frac{\boldsymbol{q}}{2}\frac{\boldsymbol{q}}{2}}(3\epsilon_D(\boldsymbol{q}_0) - \epsilon_\mu(\boldsymbol{q}_0-\boldsymbol{q}), 2\boldsymbol{q}_0+\boldsymbol{q})$ arise from the kinematically allowed loss processes into free polaritons discussed in the main text, which occur at large q_z.

To more explicitly demonstrate the exponential suppression of these contributions near the inflection point we note that the two-body T-matrix can be found from the Lippmann-Schwinger equation for Rydberg polaritons generalized to include the transverse momentum [S3]

$$T_{\boldsymbol{k}\boldsymbol{k}'}(\omega, \boldsymbol{K}) = V_{\boldsymbol{k}-\boldsymbol{k}'} + \int \frac{d^3q}{(2\pi)^3} V_{\boldsymbol{k}-\boldsymbol{q}} g^{\boldsymbol{q}}_{ss}(\omega, \boldsymbol{K}) T_{\boldsymbol{q}\boldsymbol{k}'}(\omega, \boldsymbol{K}), \tag{S15}$$

$$g^{\boldsymbol{q}}_{ss}(\omega, \boldsymbol{K}) = \sum_{\mu,\nu} \frac{|S^{\boldsymbol{K}/2+\boldsymbol{q}}_\mu|^2 |S^{\boldsymbol{K}/2-\boldsymbol{q}}_\nu|^2}{\omega - \epsilon_\mu(\boldsymbol{K}/2+\boldsymbol{q}) - \epsilon_\nu(\boldsymbol{K}/2-\boldsymbol{q}) + i\epsilon}, \tag{S16}$$

where $g^{\boldsymbol{q}}_{ss}(\omega, \boldsymbol{K})$ is the non-interacting, time-ordered Green's function for two Rydberg states.

For relative momenta q_z much larger than $g^2/c\Delta$, $g^{\boldsymbol{q}}_{ss}(\omega, \boldsymbol{K})$ saturates to the constant

$$\bar{\chi}(\omega) = \lim_{|q_z|\to\infty} g^{\boldsymbol{q}}_{ss}(\omega, \boldsymbol{K}) \tag{S17}$$

which implies that the T-matrix for large longitudinal momentum transfers approaches $T_{\boldsymbol{k}\boldsymbol{k}'}(\omega, \boldsymbol{K}) \approx U_{\boldsymbol{k}-\boldsymbol{k}'}/\alpha$, where $U_{\boldsymbol{k}} = \int d^3r e^{i\boldsymbol{k}\cdot\boldsymbol{r}} U(\boldsymbol{r})$ and $U(\boldsymbol{r})$ is defined in Eq. (1) of the main text.

From the analysis in the main text we know that, in the absence of two-body bound states, the three-body resonances in Eq. (S14) are associated with large virtual momentum q_z. This implies that the three-body loss will be exponentially suppressed by the term $[T^s_{0\boldsymbol{q}}(2\epsilon_D(\boldsymbol{q}_0), 2\boldsymbol{q}_0)]^2 \approx |U_{\boldsymbol{q}}|^2/\alpha^2$ evaluated at the resonant values of $\boldsymbol{q}$. Near the inflection point there is an additional suppression of the three-body loss from the overlap factor with the incoming and outgoing dark-state polaritons $|S^{\boldsymbol{q}_0}_D|^6 \approx \Omega^2/\Delta^2$.

III. PERTURBATIVE INCLUSION OF MASS ANISOTROPY

In this section, we introduce an approximation method that includes the effect of the anisotropic mass by treating the coupling to the higher-partial waves in the rescaled coordinates perturbatively.

In the rescaled coordinates, the multichannel potential matrix $U_{\ell\ell'}(r)$ [see Eq. (S6)] fully describes anisotropic

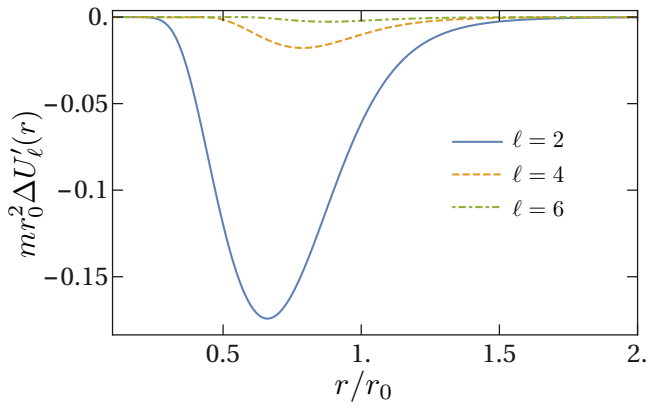

FIG. S3: Each non-zero term $\Delta U'_\ell(r)$ in the perturbative correction to the potential $U_{00}(r)$ due to anisotropic interactions. We show the range $\ell = 0 - 6$. The mass ratio $m_\perp/m_z = 10$.

interactions on the two-body level. In principle, a numerically exact treatment of the three-body scattering problem requires this multichannel two-body potential, including all partial waves. However, we can most simply describe the qualitative affect of anisotropic interactions on important three-body physics, like the Efimov effect, using a single-channel two-body potential. To this end we use a two-body model potential $U'(r)$ that perturbatively includes the affect of anisotropic interactions.

For isotropic interactions the potential matrix $U_{\ell\ell'}(r)$ becomes diagonal, and we can fully describe low-energy scattering using only the s-wave ($\ell = 0$) potential. We find corrections to this potential due to anisotropic interactions using second-order perturbation theory in an approximation that only captures s-wave resonances [S1],

$$U'(r) = U_{00}(r) - \sum_{\ell\neq 0}^{\ell_{\max}} \frac{U_{0\ell}^2(r)}{U_{\ell\ell}(r) - U_{00}(r)}, \tag{S18}$$

where the value $\ell_{\max}$ identifies the highest partial wave included in the model potential $U'(r)$. This potential can be numerically converged by taking the limit $\ell_{\max} \to \infty$.

The terms of the sum on the right hand side of equation (S18) decrease rapidly with increasing l. We define each term as

$$\Delta U'_\ell(r) = -\frac{U_{0\ell}^2(r)}{U_{\ell\ell}(r) - U_{00}(r)}. \tag{S19}$$

We show each non-zero term from $\ell = 0 - 6$ in Fig. S3, where only even partial waves couple to the s-wave channel. For $\ell > 6$ each term is essentially zero for all r on this scale.

In order to study Efimov physics we tune the depth of our model potential $U'(0)$ such that a two-body bound state resides at zero energy and the scattering length of this potential diverges. For each choice of $\ell_{\max}$ this resonant depth is slightly different. Table I shows these depths for a mass ratio $m_\perp/m_z = 10$. We see that the depth converges quickly as a function of $\ell_{\max}$ and that the addition of $\Delta U'_6(r)$ makes less than a 0.1% change in the depth. Therefore, we neglect contributions to $U'(r)$ from channels of partial-wave character greater than $\ell = 6$. Furthermore, the position of the first scattering resonance computed using this approximation agrees with the non-perturbative calculations presented in Fig. 2(c) of the main text and in Sec. I. We choose $\ell_{\max} = 6$ to construct the model potential $U'(r)$, and we compute three-body potentials using this model. Although an accurate description of the three-body physics requires the full treatment of the anisotropic character of the two-body interactions, our simple model is able to qualitatively describe the dependence of Efimov physics on the strength of the anisotropy (see, for instance, Ref. [S4])

TABLE I: The depth of the potential $U'(r)$ that supports a zero-energy bound state, for each value of $\ell_{\max}$. The mass ratio $m_\perp/m_z = 10$.

$\ell_{\max}$	$\sqrt{-mU'(0)}r_0$
0	2.3339
2	2.2705
4	2.2645
6	2.2635

IV. EXPERIMENTAL REQUIREMENTS TO REALIZE LONG-LIVED EFIMOV STATES

The two primary requirements to realize long-lived Efimov trimers of Rydberg polaritons are given by Eq. (7) and Eq. (12) in the main text. Three other important considerations are (i) the size of the Efimov state does not exceed the size of the atomic cloud, (ii) the atomic density is low enough to avoid molecular Rydberg state effects [S5, S6, S7, S8] and (iii) the thermal motion of the atoms does not break up the Efimov states. The first requirement is of particular relevance for small values of β because, when the coordinates are transformed back to the lab-coordinates, we see that the longitudinal size of the Efimov states will scale as $r_0 \approx r_b/\beta$. For an atomic density of 10^{13} cm^{-3}, we require $\beta < 0.1$, which implies that the length of the atomic cloud should be greater than 100 μm. For these densities the mean inter-atomic spacing is around 0.5 μm. To avoid collisions between the Rydberg electron and other ground state atoms, this places an upper bound on the Rydberg quantum number in the range of $n = 50 - 100$. In the case of ^{87}Rb this leads to $r_b \approx 5 - 15$ μm, for which the first polariton scattering resonance [see Fig. 2(c) in the main text] is readily achievable at these densities. To neglect motional dephasing of the atoms we require that the doppler broadening of the two-photon transition is much less than the binding energy of Efimov states. For the case of ^{87}Rb at a temperature of 35 μK, the doppler broadening is on the order of 100 kHz, while the Efimov binding energy

scales as Ω^2/Δ, which can be much larger than 1 MHz depending on parameters.

[S1] J. L. Bohn, M. Cavagnero, and C. Ticknor, *Quasi-universal dipolar scattering in cold and ultracold gases*, New J. Phys. **11**, 055039 (2009).

[S2] E. Braaten and H. W. Hammer, *Three-Body Recombination into Deep Bound States in a Bose Gas with Large Scattering Length*, Phys. Rev. Lett. **87**, 160407 (2001).

[S3] P. Bienias, S. Choi, O. Firstenberg, M. F. Maghrebi, M. Gullans, M. D. Lukin, A. V. Gorshkov, and H. P. Büchler, *Scattering resonances and bound states for strongly interacting Rydberg polaritons*, Phys. Rev. A **90**, 053804 (2014).

[S4] Y. Wang, J. P. D'Incao, and C. H. Greene, *Efimov effect for three interacting bosonic dipoles*, Phys. Rev. Lett. **106**, 233201 (2011).

[S5] J. B. Balewski, A. T. Krupp, A. Gaj, D. Peter, H. P. Büchler, R. Löw, S. Hofferberth, and T. Pfau, *Coupling a single electron to a Bose-Einstein condensate*, Nature **502**, 664 (2013).

[S6] A. Derevianko, P. Kómár, T. Topcu, R. M. Kroeze, and M. D. Lukin, *Effects of molecular resonances on rydberg blockade*, Phys. Rev. A **92**, 063419 (2015).

[S7] J. D. Thompson, T. L. Nicholson, Q.-Y. Liang, S. H. Cantu, A. V. Venkatramani, S. Choi, I. A. Fedorov, D. Viscor, T. Pohl, M. D. Lukin, et al., *Symmetry-protected collisions between strongly interacting photons*, Nature **542**, 206 (2017).

[S8] H. Busche, P. Huillery, S. W. Ball, T. Ilieva, M. P. A. Jones, and C. S. Adams, *Contactless nonlinear optics mediated by long-range Rydberg interactions*, Nature Phys. **13**, 655 (2017).